The Astrophysical Journal, 669:1143–1149, 2007 November 10

CONSTRAINTS ON THE STEADY AND PULSED VERY HIGH ENERGY GAMMA-RAY EMISSION FROM OBSERVATIONS OF PSR B1951+32/CTB 80 WITH THE MAGIC TELESCOPE

J. Albert,[1] E. Aliu,[2] H. Anderhub,[3] P. Antoranz,[4] A. Armada,[2] C. Baixeras,[5] J. A. Barrio,[4] H. Bartko,[6] D. Bastieri,[7] J. K. Becker,[8] W. Bednarek,[9] K. Berger,[1] C. Bigongiari,[7] A. Biland,[3] R. K. Bock,[6,7] P. Bordas,[10] V. Bosch-Ramon,[10] T. Bretz,[1] I. Britvitch,[3] M. Camara,[4] E. Carmona,[6] A. Chilingarian,[11] J. A. Coarasa,[6] S. Commichau,[3] J. L. Contreras,[4] J. Cortina,[2] M. T. Costado,[12] V. Curtef,[8] V. Danielyan,[11] F. Dazzi,[7] A. De Angelis,[13] C. Delgado,[12] R. de los Reyes,[4] B. De Lotto,[13] E. Domingo-Santamaría,[2] D. Dorner,[1] M. Doro,[7] M. Errando,[2] M. Fagiolini,[14] D. Ferenc,[15] E. Fernández,[2] R. Firpo,[2] J. Flix,[2] M. V. Fonseca,[4] L. Font,[5] M. Fuchs,[6] N. Galante,[6] R. García-López,[12] M. Garczarczyk,[6] M. Gaug,[7] M. Giller,[9] F. Goebel,[6] D. Hakobyan,[11] M. Hayashida,[6] T. Hengstebeck,[16] A. Herrero,[12] K. Hirotani,[17] D. Höhne,[1] J. Hose,[6] C.-C. Hsu,[6] P. Jacon,[9] T. Jogler,[6] R. Kosyra,[6] D. Kranich,[3] R. Kritzer,[1] A. Laille,[15] E. Lindfors,[18] S. Lombardi,[7] F. Longo,[13] J. López,[2] M. López,[4] E. Lorenz,[3,6] P. Majumdar,[6] G. Maneva,[19] K. Mannheim,[1] O. Mansutti,[13] M. Mariotti,[7] M. Martínez,[2] D. Mazin,[6] C. Merck,[6] M. Meucci,[14] M. Meyer,[1] J. M. Miranda,[4] R. Mirzoyan,[6] S. Mizobuchi,[6] A. Moralejo,[2] D. Nieto,[4] K. Nilsson,[18] J. Ninković,[6] E. Oña-Wilhelmi,[2] N. Otte,[6,16,20], I. Oya,[4] D. Paneque,[6] M. Panniello,[12] R. Paoletti,[14] J. M[a]. Paredes,[10] M. Pasanen,[18] D. Pascoli,[7] F. Pauss,[3] R. Pegna,[14] M. Persic,[13,21] L. Peruzzo,[7] A. Piccioli,[14] M. Poller,[1] E. Prandini,[7] N. Puchades,[2] A. Raymers,[11] W. Rhode,[8] M. Ribó,[10] J. Rico,[2] M. Rissi,[3] A. Robert,[5] S. Rügamer,[1] A. Saggion,[7] A. Sánchez,[5] P. Sartori,[7] V. Scalzotto,[7] V. Scapin,[13] R. Schmitt,[1] T. Schweizer,[6] M. Shayduk,[6,16,] K. Shinozaki,[6] S. N. Shore,[22] N. Sidro,[2] A. Sillanpää,[18] D. Sobczyńska,[9] A. Stamerra,[14] L. S. Stark,[3] L. Takalo,[18] P. Temnikov,[19] D. Tescaro,[2] M. Teshima,[6] N. Tonello,[6] D. F. Torres,[2,23] N. Turini,[14] H. Vankov,[19] V. Vitale,[13] R. M. Wagner,[6] T. Wibig,[9] W. Wittek,[6] F. Zandanel,[7] R. Zanin,[2] and J. Zapatero[5]

Received 2007 February 2; accepted 2007 July 23

ABSTRACT

We report on very high energy γ-ray observations with the MAGIC Telescope of the pulsar PSR B1951+32 and its associated nebula, CTB 80. Our data constrain the cutoff energy of the pulsar to be less than 32 GeV, assuming the pulsed γ-ray emission to be exponentially cut off. In the case that the cutoff follows a superexponential behavior, the cutoff energy can be as high as $\sim$60 GeV. The upper limit on the flux of pulsed γ-ray emission above 75 GeV is 4.3×10^{-11} photons cm^{-2} s^{-1}, and the upper limit on the flux of steady emission above 140 GeV is 1.5×10^{-11} photons cm^{-2} s^{-1}. We discuss our results in the framework of recent model predictions and other studies.

Subject headings: acceleration of particles — gamma rays: observations — pulsars: individual (PSR B1951+32) — radiation mechanisms: nonthermal

1. INTRODUCTION

It is currently believed that pulsars are among the few objects in our Galaxy that are candidate sources of ultrarelativistic charged cosmic rays. Relativistic particles within the magnetosphere emit γ-rays at energies up to several GeV in various processes such as curvature radiation, synchrotron radiation, and inverse Compton (IC) scattering. Thus, observations in the multi-GeV γ-ray domain allow one to study the acceleration sites in the magnetosphere of a pulsar. Predicted sites where particle acceleration can take place are, for example, above the polar cap of the neutron star (e.g., Harding et al. 1978; Daugherty & Harding 1982) and in the so-called outer gap of the magnetosphere (e.g., Cheng et al. 1986a, 1986b; Chiang & Romani 1992). Furthermore, particle acceleration can take place outside the magnetosphere in the region where the pulsar wind interacts with the interstellar medium. If electrons are accelerated in these shocks, they could give rise to IC-scattered photons from, for example, the cosmic microwave background, synchrotron radiation, or a thermal origin (de Jager & Harding 1992; Atoyan & Aharonian 1996; Bednarek & Bartosik 2003).

[1] Universität Würzburg, D-97074 Würzburg, Germany.
[2] Institut de Física d'Altes Energies, Edifici Cn., E-08193 Bellaterra (Barcelona), Spain.
[3] ETH Zürich, CH-8093 Zurich, Switzerland.
[4] Universidad Complutense, E-28040 Madrid, Spain.
[5] Universitat Autònoma de Barcelona, E-08193 Bellaterra, Spain.
[6] Max-Planck-Institut für Physik, D-80805 Munich, Germany.
[7] Università di Padova and INFN, I-35131 Padua, Italy.
[8] Universität Dortmund, D-44227 Dortmund, Germany.
[9] University of Łódź, PL-90236 Lodz, Poland.
[10] Universitat de Barcelona, E-08028 Barcelona, Spain.
[11] Yerevan Physics Institute, AM-375036 Yerevan, Armenia.
[12] Instituto de Astrofísica de Canarias, E-38200 La Laguna, Tenerife, Spain.
[13] Università di Udine and INFN Trieste, I-33100 Udine, Italy.
[14] Università di Siena and INFN Pisa, I-53100 Siena, Italy.
[15] University of California, Davis, CA 95616-8677.
[16] Humboldt-Universität zu Berlin, D-12489 Berlin, Germany.
[17] ASIAA/National Tsing Hua University–TIARA, P.O. Box 23-141, Taipei, Taiwan.
[18] Tuorla Observatory, Turku University, FI-21500 Piikkiö, Finland.
[19] Institute for Nuclear Research and Nuclear Energy, BG-1784 Sofia, Bulgaria.
[20] Author to whom correspondence should be addressed; otte@mppmu.mpg.de.
[21] INAF/Osservatorio Astronomico and INFN Trieste, I-34131 Trieste, Italy.
[22] Università di Pisa and INFN Pisa, I-56126 Pisa, Italy.
[23] ICREA and Institut de Ciències de l'Espai, IEEC-CSIC, E-08193 Bellaterra, Spain.

PSR B1951+32 was detected first at radio frequencies by Kulkarni et al. (1988) and is one of the six rotation-powered high-energy pulsars whose GeV emission was detected by EGRET (Ramanamurthy et al. 1995). Among γ-ray pulsars, PSR B1951+32 is the only source observed to emit up to 20 GeV with no cutoff being evident in the differential energy spectrum. The spectrum shows a hard spectral index of 1.8 between 100 MeV and 20 GeV. The pulsar has an apparent high efficiency ($\sim$0.4%) of converting its rate of rotational energy loss, 3.7×10^{36} ergs s^{-1}, into γ-rays above 100 MeV (assuming a distance of 2.5 kpc to the pulsar). Moreover, the γ-ray luminosity at $\sim$10 GeV is comparable to that of the Crab pulsar (Ramanamurthy et al. 1995).

As inferred from its rotational parameters, the spin-down age of PSR B1951+32 is $\sim 10^5$ yr (Manchester et al. 2005),[24] that is, about 100 times older than the Crab pulsar. The magnetic field strength of 4.9×10^{11} G (Manchester et al. 2005) is lower than that in most rotation-powered pulsars. Because of the lower magnetic field, curvature γ-rays emitted near the stellar surface, as predicted in polar-cap models, are less affected by magnetic pair production. Compared with younger, more strongly magnetized pulsars, the spectral cutoff energy is thereby shifted to higher energies, up to a few tens of GeV (Harding 2001; Baring 2004; see also Bulik et al. 2000 for a discussion of low-field millisecond pulsars).

On the contrary, if the γ-rays are emitted in the outer magnetosphere, as predicted in outer-gap models, the potential drop in the outer gap of PSR B1951+32 is expected to be comparable to that of young pulsars (see eq. [12] of Zhang & Cheng 1997 and eq. [2.1] of Cheng et al. 1986a). Therefore, the cutoff energy, which reflects the maximum Lorentz factor of the electrons or positrons accelerated in the outer gap, is expected to be around 10 GeV (Hirotani 2007). Thus, features in the predicted spectral shape of weakly magnetized pulsars at energies above 10 GeV are strongly dependent on the emission altitude. In order to discriminate between emission models, PSR B1951+32 is a prime candidate for observation by ground-based γ-ray detectors with low energy thresholds such as the imaging air Cerenkov telescope MAGIC.

This pulsar is located in the core of the radio nebula CTB 80, which is thought to be physically associated with the pulsar. In X-rays the nebula shows a cometary shape (Moon et al. 2004; Li et al. 2005), being confined by a bow shock that is produced by the pulsar's high proper motion (240 ± 40 km s^{-1}; Migliazzo et al. 2002). Bednarek & Bartosik (2005b) predict an over–200 GeV flux from the nebula at a level of $\sim$4.4% of the Crab's flux, by assuming that high-energy leptons can accumulate inside the well-localized nebula for long periods of time, as observed in the case of the Crab Nebula.

The current tightest constraint on the emission above 100 GeV from the pulsar and its nebula, obtained by the Whipple collaboration (Srinivasan et al. 1997), puts an upper limit of 75 GeV on the cutoff energy of the pulsed emission and an upper limit of 1.95×10^{-11} cm^{-2} s^{-1} on the steady emission above 260 GeV. The latter is within a factor of $\sim$2 of the prediction of Bednarek & Bartosik (2005b).

In this paper, we present upper limits on the cutoff energy of the pulsed emission from the pulsar, as well as on the steady and pulsed very high energy (VHE) fluxes from the region associated with the radio nebula, resulting from MAGIC Telescope observations that were performed in 2006 July through September. The paper is structured as follows: After a short introduction to MAGIC and our data taking and analysis (§ 2), we report on our search for steady and pulsed emission from PSR B1951+32 (§ 3). We close with a discussion of the implications of our results (§ 4).

[24] See http://www.atnf.csiro.au/research/pulsar/psrcat.

TABLE 1
Summary of the Observations of PSR B1951+32

Date (2006)	Rate (Hz)	ON Time (minutes)	Extinction (mag)	Extinction Scatter (mag)	Selected?
Jul 4.....	164	130	0.099	0.017	Yes
Jul 5.....	164	136	0.100	0.011	Yes
Jul 6.....	167	105	0.088	0.014	Yes
Jul 7.....	176	62	0.091	0.011	Yes
Aug 3	151	95	0.161	0.009	Yes
Aug 4	...	...	0.266	0.045	No
Aug 23	175	168	0.079	0.017	Yes
Aug 24	158	105	0.088	0.014	Yes
Aug 25	165	138	0.142	0.029	Yes
Aug 26	135	148	0.168	0.044	No
Aug 27	167	124	0.140	0.042	Yes
Aug 28	...	...	0.249	0.056	No
Sep 13	147	83	...	...	Yes
Sep 14	139	155	0.105	0.016	Yes
Sep 15	156	102	0.091	0.017	Yes
Sep 16	147	125	0.095	0.013	Yes
Sep 17	149	89	0.094	0.060	Yes

Notes.—The extinction coefficients are taken from publicly available data from the Carlsberg Meridian Telescope, which is located on the same site as MAGIC. The extinction coefficient is for an effective wavelength of 625 nm.

2. OBSERVATIONS AND ANALYSIS

The MAGIC (Major Atmospheric Gamma Imaging Cherenkov) Telescope (see Lorenz 2004) is located on the Canary Island of La Palma (2200 m above sea level, 28.45°N, 17.54°W). MAGIC is currently the largest imaging atmospheric Cerenkov telescope, having a 17 m diameter tessellated reflector dish comprising 964, 0.5×0.5 m^2 diamond-milled aluminum mirrors. The faint Cerenkov light flashes produced by air showers are recorded by the telescope camera, which consists of 577 photomultiplier tubes. Together with the current configuration of the MAGIC camera, with a trigger region of 2.0° diameter (Cortina et al. 2005), this results in a trigger collecting area for γ-rays of about 10^5 m^2 at small zenith angles. The effective collecting area depends on the analysis and is $\sim 10^4$ m^2 around 60 GeV and increases to $\gtrsim 6 \times 10^4$ m^2 beyond 200 GeV. At present, the minimum trigger energy is 50–60 GeV (at small zenith angles). The MAGIC Telescope is focused to 10 km distance—the most likely position for a 50 GeV air shower maximum. The accuracy in reconstructing the direction of incoming γ-rays on an event-by-event basis (point-spread function) is about 0.1°, depending on energy and the chosen analysis method. A source with a γ-ray flux of $\sim$2% that of the Crab Nebula and the same spectral slope can be detected by MAGIC above 200 GeV at a significance level of 5 σ within 50 hr.

PSR B1951+32 was observed with MAGIC for a total of 17 nights between 2006 July 4 and September 17. The observations were performed in the so-called ON/OFF mode; that is, PSR B1951+32 was observed by directly pointing to it (ON). Three nights were rejected because of unstable trigger rates due to bad weather. The background was estimated by observing at the same range of zenith angle for 5.8 hr a suitable region in the sky where no γ-ray source is expected (OFF). In total, 30.7 hr of data were processed. The zenith-angle range of the observation was restricted to between 5° and 25°, guaranteeing the lowest possible

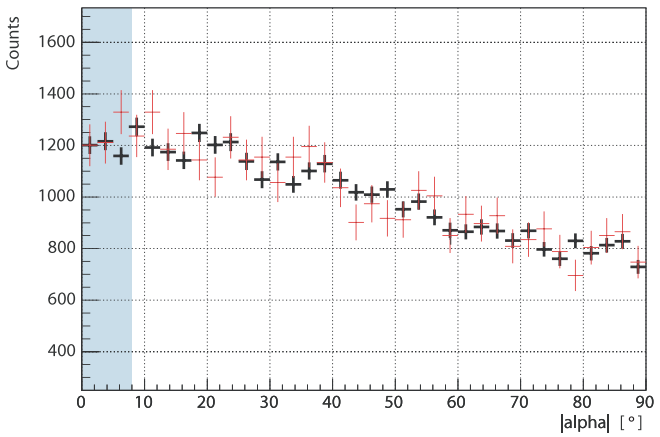

FIG. 1.—Distribution of the parameter |alpha| for events ≳280 GeV. The distribution of OFF-source events (*red*) was normalized to the ON-source events (*black*) between 20° and 85°. An excess due to γ-rays from PSR B1951+32 is expected for |alpha| < 7.5° (*shaded region*).

energy threshold. A summary of the observations is given in Table 1. This table also includes the atmospheric extinction coefficients for all nights, provided by the Carlsberg Meridian Telescope, which is located at the same site as MAGIC.

Following calibration of the data (Gaug et al. 2005) and a tail-cut image cleaning of the events, a Hillas parameterization algorithm was applied (Hillas 1985). The tail cuts used in the image cleaning were 6 photoelectrons for core pixels and 4 photoelectrons for boundary pixels. For the generation of sky maps, we used tail cuts of 10 and 5 photoelectrons. Additional suppression of pixels containing noise was achieved by requiring a narrow time coincidence between adjacent pixels (∼7 ns). The hadronic background was suppressed with a multivariate method, random forests (Breiman 2001; Bock et al. 2004), which uses the Hillas parameters of an event to decide on its so-called hadronness. The power to suppress hadronic background is energy dependent and reduced for γ-ray energies below 150 GeV. As a consequence, the optimal cut in hadronness, which gives the highest rejection of background while retaining most γ-ray candidates, has to be independently determined for each energy region. For the analysis of the data presented here, we used an energy-dependent hadronness cut, whose empirical parameterization was derived from Monte Carlo (MC) studies. An exception is the sky maps, for which a static hadronness cut was applied in the event selection. This is justified, as the maps were produced for energies above 200 GeV, where the dependence of the optimal hadronness cut on energy is small. The method of random forests is also used to estimate the energy of an event. Typically, energy resolutions of ∼25% are achieved on an event-by-event basis.

3. RESULTS

3.1. *Search for Steady Emission*

We searched for steady γ-ray emission of a point source from the direction of PSR B1951+32 with different analysis thresholds between 140 GeV and 2.6 TeV. We define the analysis threshold as the peak of the energy distribution of MC events after cuts. Images of γ-rays from PSR B1951+32 point with their major axis to the camera center and thus appear as an excess at small values in the parameter "alpha." Alpha is the angle between the major axis of the shower image and the direction determined by the image's center of gravity and the camera center. In Figure 1, we show the distribution of |alpha| for events with energies ≳280 GeV. An excess due to γ-ray emission from PSR B1951+32 should be visible in the figure for |alpha| < 7.5°. The results of this analysis and others with different analysis thresholds are summarized in Table 2. As no significant signal (>5 σ) from γ-rays was found, we calculated upper limits on the number of excess events with a confidence level of 95% by using the method of Rolke et al. (2005). In the calculation of the limits, a systematic uncertainty on the flux of 30% was taken into account. The upper limits on excess events were converted into integral flux limits by assuming a spectral index of 2.6, which is similar to the spectral index of the predictions and other known pulsar wind nebulae (PWNs) such as the Crab Nebula. If a harder spectrum with index 2.0 is assumed, the flux limits increase by about 15%, and they decrease by about 40% if a softer spectrum with index 4.0 is assumed. The integral flux limits of γ-rays are shown in Figure 2 together with the measurement of Srinivasan et al. (1997) and the predictions of Bednarek & Bartosik (2003).

3.2. *Search for γ-Ray Emission in the Vicinity of PSR B1951+32*

We explored the region in the sky around the position of the pulsar for a possible extended or displaced emission region of γ-rays. The latter is a likely scenario because of the high proper motion of the pulsar. For this study, we employed the DISP method of Fomin et al. (1994) with a modified parameterization (Domingo-Santamaría et al. 2005), which permits the reconstruction of the arrival direction of a ≳100 GeV γ-ray with an accuracy of ∼0.1°. Sky maps were produced in different bins of energy. In none of the maps was γ-ray emission found within the reconstructed field of view, of ∼0.6° radius.

The map in Figure 3 (*left*) shows the significance calculated in bins of 0.1° × 0.1° for events with energies ≳200 GeV. Figure 4 shows a map of the calculated upper limits (95% confidence level) on the integral flux for the same events. The acceptance of the MAGIC camera was modeled using the radial dependence of the background rate in the camera after event selection. By comparing with MC simulations, we confirmed for various angular

TABLE 2
RESULTS OF THE ANALYSIS SEARCHING FOR STEADY γ-RAY EMISSION FROM PSR B1951+32

Analysis Threshold (GeV)	ON Events	OFF Events	Excess Events	Significance (σ)	Upper Limit, Excess Events (95% C.L.)	Flux Upper Limit (cm^{-2} s^{-1})
>140	37869	37933 ± 381	−64	−0.2	792	1.5×10^{-11}
>280	3576	3740 ± 150	−164	−1.0	196	2.7×10^{-12}
>530	712	777 ± 42	−65	−1.3	54	7.0×10^{-13}
>800	232	231.5 ± 22	0.5	0.0	55	7.0×10^{-13}
>1060	101	90.6 ± 14	10.4	0.6	45	5.8×10^{-13}
>1400	58	49.5 ± 10.8	8.5	0.6	35	3.9×10^{-13}
>2600	17	26 ± 10	−9	−0.9	14	2.5×10^{-13}

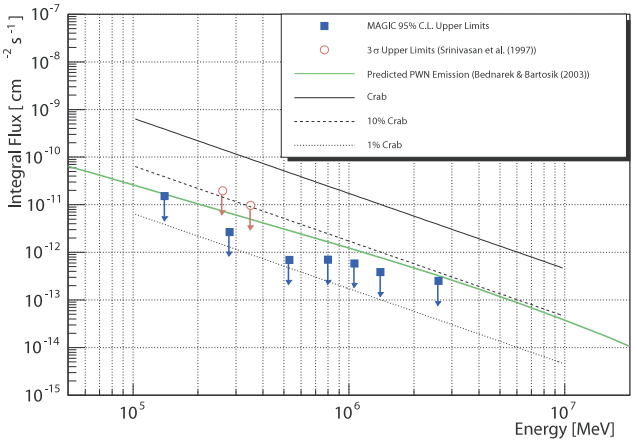

FIG. 2.—Integral upper limits (95% confidence level) on the steady γ-ray emission from the direction of PSR B1951+32. For comparison, the γ-ray flux of the Crab Nebula (Wagner et al. 2005) is also indicated.

distances from the camera center that the radial dependence of the background rate is compatible with the simulated γ-ray acceptance.

Following our study, we can exclude steady γ-ray emission above 200 GeV at the level predicted by Bednarek & Bartosik (2003), which we would have detected if (1) the emission were originating from within a circle of radius $\approx 0.4^\circ$ centered on the position of the pulsar and (2) the apparent emission region was restricted to less than $\sim 0.3^\circ$ in diameter.

3.3. *Search for Pulsed Emission*

The time of each event (hereafter "arrival time") is derived from the time signal of a GPS-controlled rubidium clock with a precision of $\sim$200 ns. Before we searched for pulsed emission from the pulsar, the arrival times were transformed to the barycenter of the solar system with the Tempo timing package, by J. H. Taylor et al.[25] Afterward, the corrected arrival times t_j were folded to the corresponding phase ϕ_j of PSR B1951+32:

$$\phi_j = \nu(t_j - t_0) + \tfrac{1}{2}\dot{\nu}(t_j - t_0)^2 + \tfrac{1}{6}\ddot{\nu}(t_j - t_0)^3,$$

where ν, $\dot{\nu}$, $\ddot{\nu}$, and t_0 are the values from a contemporary ephemeris provided by A. Lyne (2006, private communication), which is listed in Table 3. The analysis chain that was set up to search for pulsed emission was previously tested on data from an optical observation of the Crab pulsar with the central pixel of the MAGIC camera (Lucarelli et al. 2005). Details of the optical observation can be found in F. Lucarelli et al. (2007, in preparation).

We performed a search for pulsed γ-ray emission from PSR B1951+32 in five differential bins of reconstructed energy between 100 GeV and 2 TeV. To test for periodicity, we applied the Pearson χ^2 test, the H-test (de Jager et al. 1989), and a test from Gregory & Loredo (1992; a Bayesian test). No signature of pulsed emission was found in any of the energy intervals. As an example, we give the results from the H-test, which yielded significances of 0.3, 2.3, 0.6, 0.2, and 1.4 σ, respectively, with increasing energy. The corresponding 95% confidence level upper limits on pulsed emission are shown in Figure 5. The limits were calculated from the results of the H-test (de Jager 1994) by assuming a duty cycle for the pulsed emission of 36%, which corresponds to the duty cycle of PSR B1951+32 at energies above 100 MeV (Ramanamurthy et al. 1995). A spectral slope of 2.6 was assumed in the calculation of the upper flux limit. Note that these are upper limits in differential bins of energy, whereas the upper limits from Whipple (Srinivasan et al. 1997) are integral ones, which were converted to differential ones assuming a spectral shape of 2.6.

In a second analysis, we searched for pulsed emission by selecting events with SIZE > 100 photoelectrons,[26] that is, events with energies $\gtrsim$75 GeV. Again, no hint of pulsed emission was found.

[25] See http://www.atnf.csiro.au/research/pulsar/tempo.

[26] SIZE is the integrated intensity of a shower image after applied tail cuts in units of photoelectrons. It is also a good measure of the incident energy for shower impact parameters between $\sim$50 and 120 m.

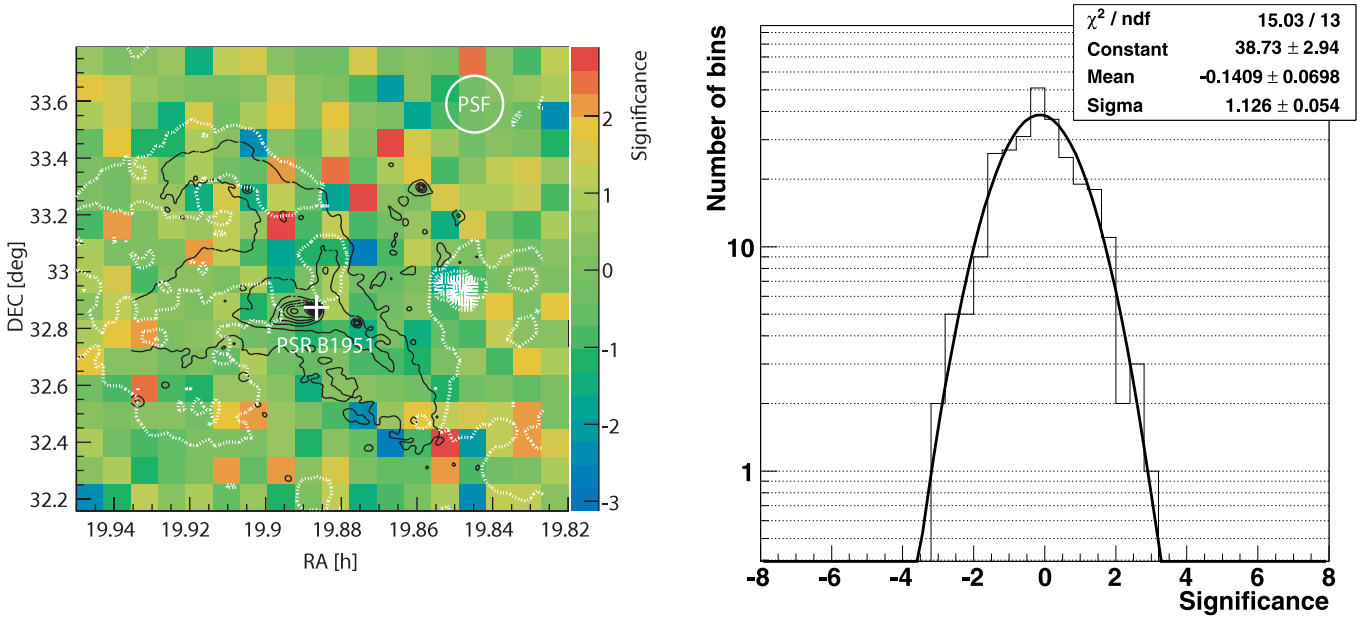

FIG. 3.—Significance of VHE γ-ray emission from the region around PSR B1951+32. *Left*: Calculated significance of VHE γ-ray emission $\gtrsim$200 GeV in bins of $0.1^\circ \times 0.1^\circ$. Overlaid in black are contours from radio observations (Castelletti et al. 2003) and in white contours from IR observations (Fesen et al. 1988). *Right*: Distribution of significances. The distribution is compatible with that of randomly distributed data.

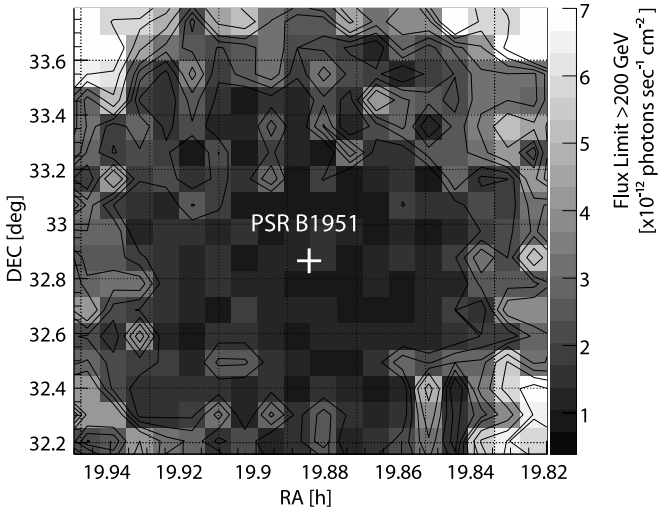

FIG. 4.—Upper limits (95% confidence level) on the integral γ-ray emission above 200 GeV, calculated in bins of $0.05^\circ \times 0.05^\circ$.

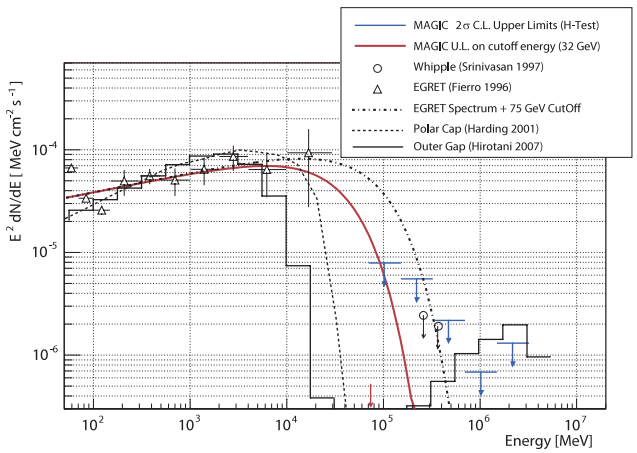

FIG. 5.—Results of the analysis in the search for pulsed emission from PSR B1951+32. Upper limits are given at the 95% confidence level. The upper limit on the cutoff energy from Whipple is shown as the dot-dashed curve. The upper limit on the cutoff of 32 GeV by MAGIC is shown as the solid red curve. The analysis threshold (75 GeV) is marked by an arrow on the horizontal axis.

The *H*-test yielded 1.4, and a χ^2 test yielded 7.2 with 11 degrees of freedom. The Bayesian test gave a probability for pulsed emission of 2.4×10^{-4}.

From the results of the *H*-test, we calculated an upper limit on the number of excess events (see Table 4), from which we derived an upper limit on the cutoff energy of the pulsed emission in the following way: The known spectrum of PSR B1951+32 at GeV energies, measured by EGRET (Fierro 1995), was multiplied by an exponential cutoff and convolved with the effective collecting area of the telescope. For a given cutoff energy, we then obtained the number of expected excess events by multiplying the result with the dead-time–corrected observation time. The upper limit on the cutoff energy was finally found by iteratively changing the cutoff energy until the number of expected excess events matched the upper limit on the number of pulsed excess events. With this procedure we obtained an upper limit on the cutoff energy of 32 GeV. The measured spectrum of PSR B1951+32 multiplied by an exponential cutoff of 32 GeV is shown in Figure 5 (*red curve*). The analysis threshold, 75 GeV, is marked by the red arrow in the figure. In the case that the rollover of the γ-ray spectrum is superexponential in shape, we constrain the cutoff energy to be below 60 GeV.

As a cross-check, the same analysis was repeated, this time by selecting all events with a SIZE < 300 photoelectrons, that is, events with energies $\lesssim$180 GeV. The resulting pulse phase profile in Figure 6 shows no evidence for pulsed emission. From this analysis, a slightly better upper limit on the cutoff energy of 28 GeV results. The analysis threshold, 60 GeV, was lower because events with a SIZE below 100 photoelectrons were also included in the analysis.

TABLE 3
EPHEMERIS OF PSR B1951+32

Parameter	Value
Position epoch (JD)	2,450,228.4144
R.A.	$19^h52^m58.27568995^s$
Decl.	$32^\circ52'40.6824033''$
Pulsar epoch (JD)	2,453,931.724208
ν (Hz)	25.29516019929(63)
$\dot{\nu}$ (Hz s^{-1})	$-3.72818(33) \times 10^{-12}$
$\ddot{\nu}$ (Hz s^{-2})	$-1.15(25) \times 10^{-21}$

NOTE.—From A. Lyne (2006, private communication). Uncertainties are given in parentheses.

4. DISCUSSION

Theoretical predictions and experimental evidence from lower energies had been quite favorable for a possible detection of γ-ray emission from PSR B1951+32 or its nebula with MAGIC. Nevertheless, despite the higher sensitivity of this observation compared with previous ones, no γ-ray emission was detected.

The upper limits in Figure 2 on the steady γ-ray emission from the PWN surrounding PSR 1951+32 are below the γ-ray flux that was predicted by the time-dependent model of Bednarek & Bartosik (2003, 2005a). Although their model takes into account the temporal evolution of the nebula (but not the spatial evolution), the acceleration of leptons and therefore also the equilibrium spectrum of leptons inside the nebula still depends on a few free parameters. These parameters, for example, the density of the medium surrounding the PWN, the acceleration efficiency of leptons, and the magnetization parameter of the pulsar wind at the shock region, are not well constrained by observations.

Concerning the magnetization parameter, that is, the ratio of the magnetic energy flux to the particle energy flux, Li et al. (2005) have recently estimated the magnetic field strength of the compact X-ray nebula around PSR B1951+32 to be $\sim$300 μG, which is larger than the value assumed by Bednarek & Bartosik. At the present time it is therefore clear that the value of the magnetization parameter σ of the pulsar wind has to be much larger than $\sigma = 10^{-3}$, which Bednarek & Bartosik assumed. As a result, the cooling of electrons by synchrotron radiation is faster and the IC γ-ray flux is suppressed. Nevertheless, a hadronic component, as predicted in some models (Bednarek & Bartosik 2003; Horns et al. 2006), which would dominate if the acceleration efficiency of leptons was low (Bednarek 2007), would be below the sensitivity of our observation.

Another aspect is that the model of Bednarek & Bartosik deals with PWNs that are well confined by the external medium and pulsars that are, at most, moving slowly through the interstellar medium (the prototype of such a nebula is the Crab Nebula). Only in such a scenario should a well-localized γ-ray source be expected, whereas when a pulsar is moving very fast, the γ-ray emission

TABLE 4
Results of the Analysis for Periodicity

Excess Events (cm^{-2} s^{-1})	*H*-Test					
	Result	Significance (σ)	2 σ U.L., Excess Events	2 σ Flux U.L. (cm^{-2} s^{-1})	χ^2	Bayesian
SIZE > 100 e^-.....	1.4	0.3	2188	4.3×10^{-11}	7.2	2.4×10^{-4}
SIZE < 300 e^-.....	3.2	1.1	3388	5.0×10^{-11}	10.7	3.6×10^{-4}

will be distributed over a larger volume. In the case of PSR B1951+32, which is moving with an apparent velocity $v_{\rm PSR} = 240 \pm 40\ {\rm km\ s^{-1}}$ (Migliazzo et al. 2002), the γ-ray flux estimated by Bednarek & Bartosik (2005b) will be smeared over an area with a diameter d of at least

$$d = v_{\rm PSR}\tau_{\rm PSR} \approx 5.3 \times 10^{19}\ {\rm cm} \approx 0.5^\circ, \qquad (1)$$

assuming an age for the pulsar of $\tau_{\rm PSR} = 7 \times 10^4$ yr and a distance of 2 kpc. Such an extended emission region reduces the detection probability with MAGIC. Apart from the pulsar's motion and the diffusion of leptons, their confinement and cooling, as well as their injection rate into the interstellar medium over time, have to be taken into account. These parameters are unknown, and therefore, their influence on the extension of the γ-ray source is difficult to estimate. Assuming Bohm diffusion in a magnetic field of 3×10^{-6} G, one estimates a diffusion length of $\sim$13 pc for 100 TeV leptons during the lifetime of the pulsar (Bednarek & Bartosik 2005b). In this case the extension would marginally increase by $\sim 0.1^\circ$ beyond what is expected from the motion of the pulsar alone. If the magnetic field distribution is ordered, the diffusion can be faster and even anisotropic, leading to much larger emission regions. In this context it is interesting to note that extended TeV γ-ray sources associated with displaced pulsars were recently detected by the H.E.S.S. Collaboration (e.g., the Vela pulsar [Aharonian et al. 2006] and PSR B1823−13 [Aharonian et al. 2005]).

Considering the γ-ray emission from the pulsar, we constrain the cutoff of the pulsed emission to less than 32 GeV if the cutoff is an exponential, which is appropriate when the γ-rays are emitted more than a few neutron star radii above the surface. If photons are emitted at lower altitudes, they are subject to magnetic pair production, resulting in a stronger (superexponential) attenuation of the energy spectrum. In the latter scenario, we constrain the allowed range of cutoff energies to be $\lesssim$60 GeV. Considering further that large uncertainties govern the last spectral point measured by EGRET, it follows that the allowed energy region where the cutoff resides can be constrained to lie somewhere between 10 and 30 GeV (exponential cutoff) or up to 60 GeV (superexponential cutoff). The narrow allowed range does not leave much freedom for models. This result and the upper limits from the search in differential bins of energy are compared in Figure 5 with theoretical predictions from the polar-cap and the outer-gap model. In this figure, the dotted line represents the polar-cap predictions from Harding (2001), renormalized to the points of the EGRET spectrum. The thin solid line shows the spectrum of the latest outer-gap model (Hirotani 2007).

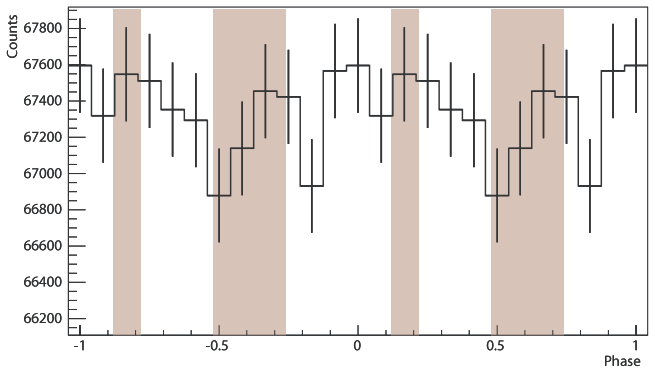

Fig. 6.—Pulse phase profile of PSR B1951+32 obtained after selecting events with SIZE < 300 photoelectrons. The shaded areas indicate the phase regions in which PSR B1951+32 is emitting at GeV energies (Ramanamurthy et al. 1995).

In polar-cap models, the cutoff energy is determined by the attenuation of γ-rays due to magnetic pair production and hence by the emission altitude of γ-rays. As a consequence, the energy spectrum above the cutoff energy is superexponentially attenuated. If the emission altitude in the polar cap model shown in Figure 5 changes from 1 to 2 stellar radii, the cutoff energy will increase from 20 to 60 GeV, which is, according to our observations, the maximum allowed cutoff energy for a superexponentially shaped cutoff. On the contrary, in outer-gap models, the cutoff is determined by the maximum Lorentz factor of the accelerated positrons and electrons. As a consequence, the cutoff of the γ-ray spectrum is smoother, resulting in an exponential cutoff. If the magnetic field lines near the light cylinder are straighter than assumed for the outer-gap spectrum in Figure 5, the predicted flux below 60 GeV will increase.

For more precise predictions of the cutoff energy in polar-cap models, multidimensional and self-consistent electrodynamics have to be examined from first principles, whereas a three-dimensional magnetic field configuration has to be investigated in the outer-gap model. Assuming that these improvements in theory will be achieved in the near future, measurements with higher statistics around 10 GeV, for example, by *GLAST*, or measurements by future ground-based experiments with lower thresholds than MAGIC, for example, MAGIC II or the Cherenkov Telescope Array, will be needed in order to distinguish between models.

The predicted IC flux at TeV energies in the outer-gap model (Fig. 5, *solid black line*) appears to be inconsistent with our upper limits. Nevertheless, it must be noted that the IC flux is obtained by assuming that all the magnetospheric soft photons illuminate the equatorial region of the magnetosphere in which the gap-accelerated positrons are migrating outward. Therefore, the predicted IC flux as a function of energy specifies an upper boundary to the possible pulsed TeV emission. The open poloidal magnetic field lines could have a single-signed curvature within 1.8 light-cylinder radii, as the solution of the time-dependent force-free electrodynamics of an oblique rotator indicates (Spitkovsky 2006). If this is the case, soft photons emitted inside the light cylinder along the convex magnetic field lines will not efficiently illuminate the magnetic field lines, which are slightly convex even outside the light cylinder. As a result, the predicted IC flux at TeV energies will be significantly reduced. This problem will be solved in the future when the self-consistent gap electrodynamics

(Hirotani 2006, 2007) and the three-dimensional force-free electrodynamics are combined.

We are grateful for the preparation of the ephemeris of PSR B1951+32 by Andrew Lyne, thus enabling us to perform the pulsed analysis. Alice Harding was so kind as to provide us with her polar-cap predictions for PSR B1951+32. We also would like to thank the Instituto de Astrofísica de Canarias for the excellent working conditions at the Observatorio del Roque de los Muchachos, in La Palma. The support of the German Bundesministerium für Bildung und Forschung and the Max-Planck-Gesellschaft, the Italian Istituto Nazionale de Fisica Nucleare, the Spanish Comisión Interministerial de Ciencias y Tecnología, ETH Research Grant TH 34/04 3, and grant 1P03D01028 from the Polish Ministerstwo Nauki i Informatyzacji are gratefully acknowledged.

REFERENCES

Aharonian, F., et al. 2006, A&A, 448, L43
Aharonian, F. A., et al. 2005, A&A, 442, L25
Atoyan, A. M., & Aharonian, F. A. 1996, MNRAS, 278, 525
Baring, M. G. 2004, Adv. Space Res., 33, 552
Bednarek, W. 2007, Ap&SS, 309, 179
Bednarek, W., & Bartosik, M. 2003, A&A, 405, 689
———. 2005a, in AIP Conf. Proc. 745, High Energy Gamma-Ray Astronomy, ed. F. A. Aharonian, H. J. Völk, & D. Horns (Melville, NY: AIP), 329
———. 2005b, J. Phys. G, 31, 1465
Bock, R. K., et al. 2004, Nucl. Instrum. Methods Phys. Res. A, 516, 511
Breiman, L. 2001, Machine Learning, 45, 5
Bulik, T., Rudak, B., & Dyks, J. 2000, MNRAS, 317, 97
Castelletti, G., Dubner, G., Golap, K., Goss, W. M., Velázquez, P. F., Holdaway, M., & Rao, A. P. 2003, AJ, 126, 2114
Cheng, K. S., Ho, C., & Ruderman, M. 1986a, ApJ, 300, 500
———. 1986b, ApJ, 300, 522
Chiang, J., & Romani, R. W. 1992, ApJ, 400, 629
Cortina, J., et al. 2005, Proc. 29th Int. Cosmic-Ray Conf. (Pune), 5, 359
Daugherty, J. K., & Harding, A. K. 1982, ApJ, 252, 337
de Jager, O. C. 1994, ApJ, 436, 239
de Jager, O. C., & Harding, A. K. 1992, ApJ, 396, 161
de Jager, O. C., Swanepoel, J. W. H., & Raubenheimer, B. C. 1989, A&A, 221, 180
Domingo-Santamaría, E., Flix, J., Rico, J., Scalzotto, V., & Wittek, W. 2005, Proc. 29th Int. Cosmic-Ray Conf. (Pune), 5, 363
Fesen, R. A., Saken, J. M., & Shull, J. M. 1988, Nature, 334, 229
Fierro, J. M. 1995, Ph.D. thesis, Stanford Univ.
Fomin, V. P., Stepanian, A. A., Lamb, R. C., Lewis, D. A., Punch, M., & Weekes, T. C. 1994, Astropart. Phys., 2, 137
Gaug, M., Bartko, H., Cortina, J., & Rico, J. 2005, Proc. 29th Int. Cosmic-Ray Conf. (Pune), 5, 375
Gregory, P. C., & Loredo, T. J. 1992, ApJ, 398, 146
Harding, A. K. 2001, in AIP Conf. Proc. 558, High Energy Gamma-Ray Astronomy, ed. F. A. Aharonian & H. J. Völk (Melville, NY: AIP), 115
Harding, A. K., Tademaru, E., & Esposito, L. W. 1978, ApJ, 225, 226
Hillas, A. M. 1985, Proc. 19th Int. Cosmic-Ray Conf. (La Jolla), 3, 445
Hirotani, K. 2006, ApJ, 652, 1475
———. 2007, ApJ, 662, 1173
Horns, D., Aharonian, F., Santangelo, A., Hoffmann, A. I. D., & Masterson, C. 2006, A&A, 451, L51
Kulkarni, S. R., Clifton, T. C., Backer, D. C., Foster, R. S., & Fruchter, A. S. 1988, Nature, 331, 50
Li, X.-H., Lu, F.-J., & Li, T.-P. 2005, ApJ, 628, 931
Lorenz, E. 2004, NewA Rev., 48, 339
Lucarelli, F., et al. 2005, Proc. 29th Int. Cosmic-Ray Conf. (Pune), 5, 367
Manchester, R. N., Hobbs, G. B., Teoh, A., & Hobbs, M. 2005, AJ, 129, 1993, http://www.atnf.csiro.au/research/pulsar/psrcat/
Migliazzo, J. M., Gaensler, B. M., Backer, D. C., Stappers, B. W., van der Swaluw, E., & Strom, R. G. 2002, ApJ, 567, L141
Moon, D.-S., et al. 2004, ApJ, 610, L33
Ramanamurthy, P. V., et al. 1995, ApJ, 447, L109
Rolke, W. A., López, A. M., & Conrad, J. 2005, Nucl. Instrum. Methods Phys. Res. A, 551, 493
Spitkovsky, A. 2006, ApJ, 648, L51
Srinivasan, R., et al. 1997, ApJ, 489, 170
Wagner, R. M., et al. 2005, Proc. 29th Int. Cosmic-Ray Conf. (Pune), 4, 163
Zhang, L., & Cheng, K. S. 1997, ApJ, 487, 370